Mixed-Integer Dynamic Optimization for Oil-Spill Response Planning with Integration of a Dynamic Oil Weathering Model

Fengqi You[i] and Sven Leyffer

Argonne National Laboratory, 9700 South Cass Avenue, Argonne, IL 60439

An R&D Note to be submitted to *AIChE Journal*

Key words: MIDO, oil-spill response planning, transport, multi-objective optimization, MINLP

1. Introduction

Catastrophic oil spills,[1] such as the recent *Deepwater BP* oil spill in the Gulf of Mexico,[2-3] have demonstrated the importance of developing responsive and effective oil spill response planning strategies for the oil industry and the government. Although a few models have been developed for oil-spill response planning, response operations and the oil weathering process are usually considered separately.[4-6] Yet significant interactions between them exist throughout the response.[6-8] Oil-spill cleanup activities change the volume and area of the oil slick and in turn affect the oil transport and weathering process, which also affects coastal protection activities and cleanup operations (e.g., performance degradation and operational window of cleanup facilities). Therefore, it is critical to integrate the response planning model with the oil transport and weathering model, although this integration has not been addressed in the existing literature to the best of our knowledge.

The objective of this note is to develop an optimization approach for seamlessly integrating the planning of oil-spill response operations with the oil transport and weathering process. A mixed-integer dynamic optimization (MIDO) model is proposed that simultaneously predicts the time trajectories of the oil volume and slick area and the optimal response cleanup schedule and coastal protection plan, by taking into account the time-dependent oil physiochemical properties, spilled amount, hydrodynamics, weather conditions, facility availability, performance degradation, cleanup operational window, and regulatory constraints. To solve the MIDO problem, we reformulated it as a mixed-integer nonlinear programming (MINLP) problem using orthogonal collocation on finite elements. We also developed a mixed-integer linear programming (MILP) model to obtain a good starting point for solving the nonconvex MINLP problem. The application of the proposed integrated optimization approach is illustrated through a case study based on the *Deepwater BP* oil spill.

The rest of this note is organized as follows. Section 2 presents the problem statement. The detailed model formulation is given in Section 3, followed by the solution approach introduced in Section 4. In Section 5, we present computational results for the case study. Section 6 summarizes our conclusions.

[i] To whom all correspondence should be addressed. Email: you@northwestern.edu; Tel: 630-252-4669

2. Problem Statement

The problem addressed in this work can be formally stated as follows. An oil spill occurs at a specific location. The initial spill volume, constant release rate, and release duration are all known. We are also given the physical and chemical parameters of the oil and seawater, as well as the weather data, such as wind speed and temperature. There is a set of staging areas $i \in I$ along the shoreline near the spill site. Because of spreading and drift processes, the oil slick may hit the coast around staging area *i* at time *t* if the slick area is larger than $\overline{AREA}_{i,t}$, which is a given parameter in this work and can be derived from the drift process based on weather and sea conditions. A minimum length of boom $\underline{L}_i$ should be deployed in staging area *i* before the oil slick hits the corresponding coast. The maximum boom deployment rates and the unit boom deployment cost are given. Booms deployed around staging area *i* will be subject to failure after a lifetime φ_i. The major cleanup methods include mechanical cleanup and recovery (skimming), in situ burning, and chemical dispersant application; and the corresponding cleanup facilities are indexed by *m*, *b,* and *d*, respectively. The maximum number of each type of cleanup facility in each staging area and the corresponding total response time are known. The operating capacities of the cleanup facilities and the corresponding operational costs and operating conditions, as well as the time-dependent weather factors, are given. When the response operations finish, the volume of oil remaining on the sea surface should not exceed the cleanup target $\underline{V}$. The problem is to simultaneously determine the coastal protection plan and cleanup schedule in order to minimize the total response cost under a specific response time span.

3. Mixed-Integer Dynamic Optimization Model

The proposed MIDO model has an objective function to minimize the total response cost, given in (33), and includes a set of ordinary differential equations (ODEs) for the oil transport and weathering process ((1)-(14)) and a set of mixed-integer constraints for response planning ((15)-(32)). The oil weathering model uses a continuous-time representation, while in the planning model we discretize the planning horizon into $|T|$ time periods with H_t as the length of time period $t \in T$. This is consistent with the real-world practice that most response decisions are made on an hourly or daily basis. The integration of these two time representations will be discussed in Section 4. A list of indices, parameters, and variables is given in the nomenclature section.

3.1 Oil transport and weathering model

Prediction of the oil transport and weathering process needs to account for many factors, such as oil properties, spilled amount, hydrodynamics, and weather conditions, and to consider a variety of complex physicochemical processes taking place simultaneously (see Figure 1). Over 50 oil weathering models, based on empirical and semi-empirical approaches, have been developed. Although any oil weathering model can, in principle, be used in the approach proposed in this paper, we employ a dynamic mathematical model taking into account the dominant processes (spreading, evaporation, emulsification, and dispersion) that cause significant short-term changes in oil characteristics. We note that a PDE model might better capture the physiochemical evolution of oil slick in the three dimension space, it might be challenging to be integrated with the response planning model. Thus, we consider only the time variation in area, volume and other important physiochemical parameters, and model the effect of wind and current through parameters with constant values.

Spreading, which strongly influences coastal protection operations and other weathering processes, is probably the most dominant process of a spill. The rate of change of slick area is given by[9-11]

$$\frac{dA_{(t)}}{dt} = K_1 A_{(t)}^{-1} V_{(t)}^{4/3} - W_{(t)} \cdot \frac{A_{(t)}}{V_{(t)}} \ , \tag{1}$$

where A is the surface area of oil slick (m^2), V is the volume of oil (m^3), and K_1 is the physicochemical parameters of the crude oil with a default value, and W is the cleanup rate given in Equation (32). The first term on the right-hand side of Equation (1) is for the natural spreading process. The second term refers to the reduction of slick area as a result of cleanup operations. Symbols with subscript (t) are time-dependent variables.

The initial area of oil slick can be determined by the well-known gravity-viscous formulation:[12]

$$A_0 = \pi \frac{k_2^4}{k_3^2} \left[\frac{\left(\rho_w - \rho_o\right) g V_0^5}{\rho_w v_w} \right]^{1/6} \ , \tag{2}$$

where g is the acceleration of gravity (m/s^{-2}), ρ_w is seawater density, ρ_o is the density of fresh oil, v_w is the kinematic viscosity of seawater, V_0 is the initial volume, and k_2 and k_3 are empirical constants.

The volume balance of the oil slick is based on the volume variation rate given as follows:[11, 13]

$$\frac{dV_{(t)}}{dt} = -V_{(t)} \frac{dF_{E(t)}}{dt} - \frac{dV_{D(t)}}{dt} - W_{(t)} + VI_{(t)} \ , \tag{3}$$

where the first term on the right-hand side is for the evaporation loss, the second term is for natural dispersion, the third term is the cleanup rate, and the last term is the oil spill rate given as follows:[11]

$$VI_{(t)} = \begin{cases} \text{constant spill rate}, & 0 \le t \le tf_1 \\ 0, & tf_1 \le t \le tf_2 \end{cases} \ , \tag{4}$$

where tf_1 is the time when the oil spillage stops and tf_2 is the final time of the planning horizon (response time span). The initial volume of the oil slick is given as V_0, and the remaining volume of oil at the end of the response time span should not exceed the cleanup target.

$$V_{(t=0)} = V_0 \text{ and } V\left(t = tf2\right) \le \underline{V} \tag{5}$$

Evaporation is the primary initial process involved in the removal of oil from sea. The rate that oil evaporates from the sea surface is modeled by the following equation:[14]

$$\frac{dF_{E(t)}}{dt} = \frac{K_{ev}A_{(t)}}{V_{(t)}}\exp\left(A_{ev} - \frac{B_{ev}}{T_K}\left(T_o + T_G F_{E(t)}\right)\right), \tag{6}$$

where F_E is the volume fraction of oil that has been evaporated, T_K is the oil temperature (K), which is assumed to be a constant, K_{ev} is the mass transfer coefficient for evaporation, T_O is the initial boiling point, T_G is the gradient of the oil distillation curve, and A_{ev} and B_{ev} are empirical constants. As no oil was evaporated at time 0, the initial value of evaporative fraction is given by

$$F_{E(t=0)} = 0 \ . \tag{7}$$

The rate of dispersion into the water column of the floating oil slick is given by the following:[9-10, 13]

$$\frac{dV_{D(t)}}{dt} = \frac{0.11\cdot\left(WIND+1\right)^2\cdot A_{(t)}\cdot V_{(t)}}{A_{(t)} + 50\zeta_t\cdot V_{(t)}\cdot\mu_{(t)}^{1/2}} \ , \tag{8}$$

where V_D is volume of oil naturally dispersed, $WIND$ is the wind speed, and ζ_t is the oil-water interfacial tension. The initial value of the volume of oil that is naturally dispersed is zero.

$$V_{D(t=0)} = 0 \tag{9}$$

In emulsification, water droplets are entrained in the oil. The dynamic emulsification process that incorporates water into oil can be computed with the following equation:[9]

$$\frac{dY_{W(t)}}{dt} = K_{em}\cdot\left(WIND+1\right)^2\cdot\left(1-\frac{Y_{W(t)}}{C_3}\right), \tag{10}$$

where Y_W is the fractional water content in the emulsion, C_3 is a viscosity constant for the final fractional water content, and K_{em} is an empirical constant. The initial value of Y_W can be approximated to zero:

$$Y_{W(t=0)} = 0 \,. \tag{11}$$

Equations (10) and (11) yield the dynamic fractional water content of the oil slick as follows:

$$Y_{W(t)} = C_3\cdot\left[1-\exp\left(-\frac{K_{em}}{C_3}\cdot\left(WIND+1\right)^2\cdot t\right)\right] . \tag{12}$$

As a result of both Mousse formation and evaporation, the viscosity of oil slick may significantly increase during the emulsification process. The rate of changes in viscosity is given by[13, 15]

$$\frac{d\mu_{(t)}}{dt} = \frac{2.5\mu_{(t)}}{\left(1-C_3Y_{W(t)}\right)^2}\frac{dY_{W(t)}}{dt} + C_4\mu\frac{dF_{E(t)}}{dt} , \tag{13}$$

where μ is the viscosity of the oil slick and C_4 is an oil-dependent constant.

The initial value of the viscosity is the same as that of the parent oil viscosity, which can be calculated by the following equation: [15]

$$\mu_0 = 224 \times \sqrt{AC}, \tag{14}$$

where AC is the asphaltene content (%) of the parent oil.

3.2 Oil spill response planning constraints

We consider both coastal protection and oil-spill cleanup operations in the response. The major coastal protection method is to deploy booms to prevent the oil from spreading to the shore. Three major oil spill cleanup methods are mechanical cleanup and recovery, in situ burning, and chemical dispersants. Mechanical systems can skim the oil slick and recover oil from the emulsion; in situ burning and chemical dispersants remove oil only from the surface of the sea. Reviews of oil spill response methods and equipment are given by Ventikos et al.[16] and Zhong.[11]

In order to protect sensitive shorelines, either the slick area must be controlled through effective cleanup operations, or coastal protection booms must be deployed with sufficient lengths around those staging areas before they are hit by the oil slick. The following constraint models this relationship:

$$A_{(t)} \le \overline{AREA}_{i,t} + A^U \cdot z_{i,t} \qquad \forall i \in I, t \in T, \tag{15}$$

where $z_{i,t}$ is a binary variable that equals 1 if sufficient booms have been deployed to protect the shoreline around staging area i at time t, A^U is the upper bound of oil slick area, and $\overline{AREA}_{i,t}$ is a given parameter for the area of the oil slick that will hit the shore around staging area i at time period t. $\overline{AREA}_{i,t}$ depends primarily on the drift process, which relates to the wind speed and direction.[11]

The shoreline around staging area i is fully protected by the booms at time period t if and only if the length of boom is no less than the required length. So we have

$$\underline{L}_i \cdot z_{i,t} \le bl_{i,t} \le \underline{L}_i + U \cdot z_{i,t} \qquad \forall i \in I, t \in T, \tag{16}$$

where $\underline{L}_i$ is the length of boom required to protect the coast around staging area i and $bl_{i,t}$ is the length of boom deployed along the shore of staging area i at the end of time period t.

Because of currents and winds, conventional booms are subject to damages over time. Coastal protection booms deployed at staging area i can be effective for only a certain lifetime φ_i after deployment. Booms deployed at time $t-\varphi_i$ will fail at time t.[8]

$$bfail_{i,t} = bdep_{i,t-\varphi_i} \qquad \forall i \in I, t \in T \tag{17}$$

The length of the boom around the shore of staging area i at the end of time period t ($bl_{i,t}$) is equal to the boom length at the end of the previous time period ($bl_{i,t-1}$) plus the length of the boom deployed at the current time period ($bdep_{i,t}$) minus those that fail at this time period ($bfail_{i,t}$). Thus, the balance of boom length is given by the following equation.

$$bl_{i,t} = bl_{i,t-1} + bdep_{i,t} - bfail_{i,t} \qquad \forall i \in I, t \in T \tag{18}$$

The length of boom deployed along the shoreline near staging area i at time t should not exceed the maximum deployment rates ($BDU_{i,t}$) times the length of time period t (H_t). Thus, we have

$$bdep_{i,t} \le BDU_{i,t} \cdot H_t \qquad \forall i \in I, t \in T, \tag{19}$$

We define $x^M_{i,m,t}$ as the number of mechanical systems m from staging area i operating at the scene at time period t. It should not exceed the corresponding available number ($N^M_{i,m}$). None of the mechanic systems can operate before the response time ($\lambda^M_{i,m}$) to notify, mobilize, dispatch, and deploy them.

$$x^M_{i,m,t} \le N^M_{i,m} \qquad \forall i \in I, m \in M, t \in T \tag{20}$$

$$x^M_{i,m,t} = 0 \qquad t \le \lambda^M_{i,m} \tag{21}$$

The volume of oil cleaned and recovered from the sea surface with mechanical systems at time period t (W^M_t) is given by the following equation.[6]

$$W^M_t = \sum_i \sum_m \left(1 - Y_{W(t)}\right) \cdot H_t \cdot \omega^M_t \cdot Q^M_{i,m} \cdot x^M_{i,m,t} \qquad \forall t \in T, \tag{22}$$

where $Q^M_{i,m}$ is the operating capability of mechanical system m from staging area i ; ω^M_t is the weather factor (between 0 and 1), which can be determined from weather forecasting; and $Y_{W(t)}$ is the fractional water content defined in (12).

In situ burning response system b can operate only when the oil slick (δ_t) is thicker than $THICK_b$.[7] We introduce a binary variable ($xx^B_{b,t}$) to model this restriction through the following constraint:

$$THICK_b \cdot xx^B_{b,t} \le \delta_{(t)} \le THICK_b + THICK^U \cdot xx^B_{b,t} \qquad \forall i \in I, b \in B, t \in T \tag{23}$$

where $THICK^U$ is the upper bound of the slick thickness and $\delta_{(t)}$ is the thickness of the oil slick given by

$$\delta_{(t)} \cdot A_{(t)} = V_{(t)} . \tag{24}$$

For in situ burning response systems, the availability constraints are given as follows:

$$x^B_{i,b,t} \le N^B_{i,b} \cdot xx^B_{b,t} \qquad \forall i \in I, b \in B, t \in T \tag{25}$$

$$x^B_{i,b,t} = 0 \qquad t \le \lambda^B_{i,b} , \tag{26}$$

where $x^B_{i,b,t}$ is the number of in situ burning systems b from staging area i operating at the scene at time period t, $N^B_{i,b}$ is the available number in staging area i, and $\lambda^B_{i,b}$ is the corresponding response time.

The volume of oil burned at time period t (W^B_t) is given by the following equation:

$$W^B_t = \sum_i \sum_m H_t \cdot \omega^B_t \cdot Q^B_{i,b} \cdot x^B_{i,b,t} \qquad \forall t \in T, \tag{27}$$

where $Q^B_{i,b}$ is the operating capability of in situ burning system b from staging area i and ω^B_t is the weather factor for in situ burning operations at time t.

The availability constraint of chemical dispersant application systems is given by

$$x^D_{i,d,t} \le H_t \cdot \gamma_{i,d,t} \cdot N^D_{i,d} \qquad \forall i \in I, d \in D, t \in T , \tag{28}$$

$$x^D_{i,d,t} = 0 \qquad t \le \lambda^D_{i,d} \tag{29}$$

where $x^D_{i,d,t}$ is the number of sorties of chemical dispersant application systems d dispatched from staging area i at time period t, $N_{i,d}^{D}$ is the corresponding availability, and $\gamma_{i,d,t}$ is the maximum number of sorties of dispersant application systems d from staging area i to spray dispersant on the oil slick at time period t. Note that the maximum number of sorties depends on the type of dispersant application system (e.g., a helicopter may operate 10 sorties per day for an offshore oil spill 100 miles away).[17]

The volume of oil removed from the sea surface by using chemical dispersants at time period t (W_t^D) is given by the following equation:

$$W_t^D = \sum_i \sum_d \omega_t^D \cdot \rho_t^{effect} \cdot \rho_d^{accuracy} \cdot Q_{i,d}^D \cdot x_{i,d,t}^D \qquad \forall t \in T , \tag{30}$$

where $Q_{i,d}^D$ is the operating capacity of dispersant application systems d from staging area i , ω_t^D is the corresponding weather factor, ρ_t^{effect} is the effectiveness factor (ratio between oil dispersed and dispersant sprayed) for chemical dispersant application at time t, and $\rho_d^{accuracy}$ is the accuracy factor (percentage of sprayed dispersant that can reach the oil slick) of dispersant application systems d.

The total amount of chemical dispersant used throughout the entire response operation should not exceed the limit set by the regulator (*DLIMIT*).[17]

$$\sum_i \sum_d \sum_t Q_{i,d}^D \cdot x_{i,d,t}^D \le DLIMIT \tag{31}$$

We model the real-time cleanup rate ($W_{(t)}$) as a piece-wise step function as follows:

$$W_{(t)} \cdot H_t = W_t^M + W_t^B + W_t^D \ . \tag{32}$$

3.3 Objective functions

The objective function is to minimize the total response cost, given as follows.

$$\begin{aligned} \min: \ TotalCost = & \sum_i \sum_m \sum_t C_{i,m,t}^M \cdot x_{i,m,t}^M + \sum_i \sum_b \sum_t C_{i,b,t}^B \cdot x_{i,b,t}^B + \sum_i \sum_b \sum_t C_{i,d,t}^D \cdot x_{i,d,t}^D \\ & + \sum_i \sum_t CDEP_{i,t}^{boom} \cdot bdep_{i,t} - \sum_t u_t^M \cdot OC \end{aligned} \tag{33}$$

Here the first three terms are the cost of the cleanup operations, the fourth terms is the cost of coastal protection operations, and the last term is the credit resulting from the recovery of the emulsified oil. We note that another possible objective of this problem is to minimize the time span of the entire response operations,[11] which is a measure of responsiveness.[18-20]

4. Solution Approach

A number of approaches exist for solving MIDO problems.[21-29] Because of the problem size and structure, in this work we use a simultaneous approach, the robustness and efficiency of which have been demonstrated by a number of large-scale applications in process control and operations.[30-39]

4.1 Simultaneous approach for solving the MIDO problem

In the simultaneous approach,[33-34, 36, 39-40] the MIDO model is fully discretized based on orthogonal collocation on finite elements and then is reformulated into an equivalent MINLP problem. First, the entire planning horizon is divided into a number of finite elements. Within each finite element an adequate number of internal collocation points is selected. Using several finite elements is useful to represent dynamic profiles with nonsmooth variations. Thus, the differential and algebraic variable profiles are approximated at each collocation point by using a family of interpolation polynomials.

To integrate the continuous- and discrete-time representations in the model, we consider one time period as a finite element in the discretization process. In this way, the index t represents not only the discrete time periods but also the finite elements, and the length of finite element t is the same as the length of the corresponding time period (H_t). In this section we use the symbol S to generically represent the differential variables $A_{(t)}$, $F_{E(t)}$, $\mu_{(t)}$, $V_{D(t)}$, and $V_{(t)}$. Then, in the discretization process, differential equations (1), (6), (13), (8), and (3) are replaced with the following generic equations:

$$S_{t,p} = S0_t + H_t \sum_{p'=1}^{|P|} \Omega_{p',p} \cdot \dot{S}_{t,p'} \qquad \forall t \in T, p \in P, \qquad (34)$$

$$S0_t = S0_{t-1} + H_{t-1} \sum_{p=1}^{|P|} \Omega_{p,p'=|P|} \cdot \dot{S}_{t-1,p} \qquad \forall t \in T, \qquad (35)$$

$$\dot{S}_{t,p} = f\left(A_{(t)}, F_{E(t)}, \mu_{(t)}, V_{D(t)}, V_{(t)}, W_{(t)}\right) \qquad \forall t \in T, p \in P, \qquad (36)$$

where $S_{t,p}$ is the value of the state in finite element t and collocation point p, $S0_t$ is the state value at the beginning of finite element t, $\dot{S}_{t,c}$ is the first-order derivative of the state, and $\Omega_{p',p}$ is the collocation matrix. Radau collocation points are used in this work because they stabilize the system more efficiently in the presence of high-index differential algebraic equations. Equation (34) is used to compute the value of the system states at each discretized point $S_{t,p}$ by using the monomial basis representation. Equation (35) is to enforce the continuity of the differential profiles across finite elements. Equation (36) simply represents the right-hand side of the dynamic model for computing the value of the first-order derivatives of the systems.

The initial and final conditions in (2), (7), (14), (9), and (5) are replaced by the following equations:

$$S0_{t=1} = S_0 \ . \qquad (37)$$

$$S_{t=tf_2,\, p=|P|} = S_{tf_2} \ . \qquad (38)$$

The time value of each collocation point in each finite element is given by

$$TIME_{t,p} = \sum_{t'=1}^{t'=t-1} H_{t'} + H_t \cdot \Psi_p \qquad \forall t \in T, p \in P, \qquad (39)$$

where Ψ_p is the roots of the Lagrange orthogonal polynomial. This equation can be used to calculate the fractional water content in Equation (12).

After the reformulation the differential equations are discretized as in Equations (34)–(39), and the resulting problem is a nonconvex MINLP with nonlinear terms in (22), (24), and (36).

4.2 Approximate MILP model for initialization

The simultaneous approach requires careful initializations and might suffer from numerical difficulties associated with the nonlinear nonconvex terms in the reformulated MINLP. To obtain a "good" starting point, we developed a MILP model for initialization. The approximate MILP model, which is obtained by decoupling the ODE from the discrete-time response planning model, implicitly considers the oil weathering process in the response planning by assuming the time trajectory of the slick thickness is not affected by response operations.[11] First, we use the Runge–Kutta method to solve the ODE-based oil weathering model without considering response operations, that is, natural weathering with zero cleanup rate ($W_{(t)} = 0$). The oil volume, slick area, and water content predicted by the ODE model are denoted $V^*(t)$, $A^*(t)$, and $Y_W^*(t)$, respectively. Then, at each discrete time period the slick thickness can be calculated by $\delta_t^* = V^*(t) / A^*(t)$. We further define θ_t as the percentage of oil removed from the slick at time period t by natural weathering. Its value can be calculated by $\theta_t = \left[V^*(t-1) - V^*(t) + VI_t \cdot H_t \right] / V^*(t-1)$, where the term ($VI_t \cdot H_t$) accounts for the volume of oil newly released to the sea surface in time period t.

The MILP model has the same objective function given in Equation (33). The model also includes the following constraints for slick area, volume balance, and cleanup target, respectively:[11]

$$v_t = area_t \cdot \delta_t^*, \qquad \forall t \in T, \tag{40}$$

$$V_0 + VI_{t=1} \cdot H_{t=1} = v_{t=1} + \theta_{t=1} \cdot V0 + W_{t=1}^M + W_{t=1}^B + W_{t=1}^D, \tag{41}$$

$$v_{t-1} + VI_t \cdot H_t = v_t + \theta_t \cdot v_{t-1} + W_t^M + W_t^B + W_t^D, \qquad \forall t \geq 2, \tag{42}$$

$$v_{t=tf2} \leq \underline{V}, \tag{43}$$

where v_t and $area_t$ are the volume and area of the oil slick at the end of the discrete time period t, respectively.

The rest of constraints in the MILP model include (15) - (23) and (25) - (32). Note that the fractional water content $Y_{W(t)}$ in Equation (22) and the slick thickness $\delta_{(t)}$ in Equation (23) are fixed to $Y_W^*(t)$ and δ_t^*, respectively.

5. Case Study: Oil Spill in the Gulf of Mexico

Our case study is based on the *Deepwater Horizon/BP* oil spill in the Gulf of Mexico. There are three major staging areas for the response operations: S1, S2, and S3. Their locations, along with the spill site, are given in the map in Figure 3. The minimum distances between the three staging areas and the oil spill site are 60 kilometers, 120 kilometers, and 180 kilometers, respectively. In this case, we assume the oil slick drifts toward the shore as a result of wind and current directions. The lengths of the booms required to protect the sensitive coastline near the three staging areas are 200 kilometers, 180 kilometers, and 300 kilometers, respectively. The spilled oil is considered as crude oil with an API degree of 25. The initial spill amount is 10,000 m^3, and the oil releases continue for 42 days with a constant rate of 10,000 m^3/day. The cleanup target is that no more than 1,500 m^3 of oil remain on the sea surface after the response. The cleanup facilities include three types of mechanical systems, two types of in situ burning systems, and three types of dispersant application systems (vessel, helicopter, and C-130). Each system has a corresponding operating capacity, available number, operational cost, and response time. All the other input data are available upon request.

All the computational studies were performed on an IBM T400 laptop with an Intel 2.53 GHz CPU and 2 GB RAM. DICOPT was used as the MINLP solver. The MILP problems were solved by using CPLEX 12.2 with an optimality tolerance of 10^{-9}. The nonlinear programming subproblems were solved with KNITRO[41] with an optimality tolerance of 10^{-6}. In order to examine the trade-off between the total cost and the responsiveness, which is measured by the response time span,[11] we need to solve a large-scale non-convex multi-objective MINLP. Although a global optimal solution of this problem might be intractable, we use ε–constraint method[42] to obtain an approximation of the Pareto curve. We consider one day as a time period or a finite element. Because the oil volume will reduce to the cleanup target (1,500 m^3) in 180 days without cleanup actions (i.e., natural weathering) and setting the response time span less than 76 days usually leads to an infeasible solution, we solve 105 instances with a response time span ranging from 76 days to 180 days, with increments of one day. The maximum MINLP problem with a response time span of 180 days includes 3,740 discrete variables, 11,521 continuous variables, and 14,046 constraints. For each instance, we first solve the approximate MILP problem and use its solution as the starting point of solving the MINLP problem. The solution process takes a total of 15,059 CPU-seconds for all 105 instances. We note that the problem becomes "infeasible", when we solved the MINLP directly without the initialization step.

The results are given in Figures 4–11. The line in Figure 4 is the "local-optimal" Pareto curve of this problem. We can see that as the response time span increases from 76 days to 180 days, the total cost decreases from \$998 million to \$54 million. Thus, the more responsive the response operation is, the more it costs. In particular, when the response time span increases from 76 days (Point A) to 78 days (Point B), the total cost reduces almost by half. This suggests that 78 days might be a better choice for the oil spill response based on the trade-off between economics and responsiveness. The pie charts in Figure 4 are for the breakdown of the total costs for Points A–F. We can see that as the time span increases and the total cost decreases, more and more is spent on coastal protection. The reason is that the least-cost option for this case study is to deploy booms to protect the sensitive shorelines while leaving the oil slick on the sea surface until natural weathering reduces the oil volume to the cleanup target; that is, no cleanup efforts are taken in the least-cost instance.

Figures 5–7 show the time trajectories of the oil volume throughout the response operations for the Points A–C in Figure 4, where time spans are 76 days, 78 days, and 95 days. The drop lines are for the collocation points in the finite elements. We can see a similar trend from these figures that the volume of remaining oil first increases from Day 0 to Day 42 and then decreases, because the oil was being released at a constant rate to the sea surface before Day 42. These figures reveal that the more cleanup operations are taken, the earlier the cleanup target can be achieved. They also show that dispersant application is usually the most favorable cleanup method because of its flexibility in various weather conditions, although it need longer response time than other methods. In the shortest time span instance, however, skimming becomes as important as dispersant application, because the total amount of chemical dispersant used is constrained by regulation and mechanical cleanup can gain credit from oil recovery. The time trajectories of the oil volume and area when response time span is 180 days (Point F in Figure 4) are given in Figure 8. As no cleanup effort was taken in this instance, the time trajectories are the same as those for natural weathering process.

Figure 9 shows the length of coastal protection booms deployed in the three staging areas when the response time span is 76 days. We can see that the three staging areas start to deploy booms from Day 8, Day 21, and Day 19, respectively. The different starting days are due to the different boom deployment rates and different locations of the staging areas. S1 deploys the booms first, because it has shortest distance to the oil spill site; Although S2 is closer to the spill site than S3, S3 starts to deploy the booms earlier than S2, because S3 requires much longer booms to protect the coast and longer deployment time.

6. Conclusion

In this paper, we have developed an MIDO approach for oil spill response planning with integration of the physiochemical evolution of oil slicks. The MIDO model includes a dynamic oil weathering model, which takes into account the oil properties, spilled amount, hydrodynamics, and weather conditions, and models the complex interactions between the spreading, evaporation, dispersion, and emulsification processes. In addition to the time trajectories of oil volume and slick area, the MIDO model simultaneously predicts the optimal coastal protection plans and oil spill cleanup schedule with different types of mechanic, burning, and dispersant application equipment. The MIDO model was reformulated to a MINLP problem after full discretization, and an approximate MILP model was developed for the initialization of solving the large-scale, nonconvex MINLP. An example was presented to illustrate the application of the proposed integrated optimization approach. The results demonstrate the importance of integrating an oil transport and weathering model in response planning.

Acknowledgment

This research is supported by the U.S. Department of Energy under contract DE-AC02-06CH11357.

Nomenclature

Nomenclature for the planning model

Sets/Indices

B	Set of in situ burning response system types indexed by b
D	Set of chemical dispersant application system types indexed by d
I	Set of staging areas (including airlift wing stations) indexed by i
M	Set of skimming (mechanical cleanup & recovery) system types indexed by m
P	Set of collocation points indexed by p, p'
T	Set of time periods/finite elements indexed by t, t'

Parameters

$\overline{AREA}_{i,t}$	Expected slick area that the oil slick would hit the shore around staging area i at time period t if no boom in this area was deployed for protection
$BDU_{i,t}$	Maximum deployment rate of boom in staging area i at time period t
$C^{M}_{i,m,t}$	Operating cost of mechanical cleanup and recovery system m from staging area i at time t
$C^{B}_{i,b,t}$	Operating cost of in situ burning system type b from staging area i at time t
$C^{D}_{i,d,t}$	Cost of dispatching a chemical dispersant application system d from staging area i at time t to spray a full-load dispersant
$CDEP^{boom}_{i,t}$	Cost of deploying unit length of coastal protection boom in staging area i
$DLIMIT$	Maximum amount of dispersant that can be applied in the cleanup
H_t	Length of time period t
$\underline{L}_i$	Length of boom required to protect the shore around staging area i
$N^{B}_{i,b}$	Available number of in situ burning response systems of type b in staging area i
$N^{D}_{i,d}$	Available number of chemical dispersant application systems of type d in staging area i
$N^{M}_{i,m}$	Available number of mechanic systems of type m that can be dispatched from staging area i
OC	Unit price of recovered oil
$THICK_b$	Minimum slick thickness that in situ burning response system b can operate
$Q^{B}_{i,b}$	Operating capability of in situ burning system b from staging area i
$Q^{D}_{i,d}$	Full load capacity of dispersant application system d from staging area i
$Q^{M}_{i,m}$	Operating capability of mechanical cleanup system m from staging area i
$TIME_{t,p}$	Value of time at collocation point p in finite element t
V_0	Initial volume of oil spilled at time 0
VI_t	Volume of oil that was newly released to the sea surface at time t
$\underline{V}$	Cleanup target, maximum volume of oil left on the sea surface after cleanup
ρ^{effect}_t	Effectiveness factor (ratio between oil dispersed and dispersant sprayed) for chemical dispersant application operation at time t
$\rho^{accuracy}_d$	Accuracy factor (percentage of sprayed dispersant that can reach oil slick) of chemical dispersant application system d
$\lambda^{B}_{i,b}$	Total response time of in situ burning response system type b dispatched from staging area i

(including times to notify, mobilize, dispatch, and deploy the system)

$\lambda_{i,d}^{D}$ Total response time of chemical dispersant system types *d* dispatched from staging area *i*

$\lambda_{i,m}^{M}$ Total response time of mechanic cleanup and recovery system type *m* from staging area *i*

ω_t^M Weather factor for mechanic cleanup and recovery operation at time *t*

ω_t^B Weather factor for controlled burning operation at time *t*

ω_t^D Weather factor for chemical dispersant application operation at time *t*

$\gamma_{i,d,t}$ Maximum number of sorties of dispersant application system types *d* from staging area *i* to oil spill site in time period *t*

φ_i Lifetime before failure for containment booms deployed at staging area *i*

η_t Percentage of oil that can be recovered in the emulsified oil collected at time *t*

δ_t Thickness of oil slick at the end of time period *t*

θ_t Percentage of oil removed from the sea surface due to natural weathering process at time *t*

$\Omega_{p',p}$ Collocation matrix

Ψ_p Roots of the Lagrange orthogonal polynomial

Integer Variables

f_t 0-1 variable. Equal to 1 if cleanup target is not achieved at the end of time period *t*

$x_{i,m,t}^{M}$ Number of mechanical systems of type *m* from staging area *i* operating on scene at time period *t*

$x_{i,b,t}^{B}$ Number of in situ burning systems of type *b* from staging area *i* operating on scene at time period *t*

$x_{i,d,t}^{D}$ Number of sorties of dispersant application systems of type *d* dispatched from staging area *i* at time period *t* to spray dispersants

$z_{i,t}$ 0-1 variable. Equal to 1 if the shoreline around staging area *i* is protected by boom

Continuous Variables (0 to $+\infty$)

$area_t$ Area of oil slick on the surface at the end of time *t*

$bdep_{i,t}$ Amount of coastal protection booms deployed in staging area *i* at time period *t*

$bfail_{i,t}$ Amount of coastal protection booms failed in staging area *i* at time period *t*

$binv_{i,t}$ Length of available boom in staging area *i* at the end of time period *t*

$bl_{i,t}$ Length of coastal protection boom along the shore of staging area *i* at the end of time *t*

$S_{t,p}$ Value of the state in finite element *t* and collocation point *p*

$S0_t$ State value at the beginning of finite element *t*

u_t^M Volume of oil collected and recovered through mechanical systems at time *t*

u_t^B Volume of oil removed by in situ burning at time period *t*

u_t^D Volume of oil dispersed due to chemical dispersant application at time period *t*

v_t Volume of oil on the surface at the end of time *t*

Continuous Variables ($-\infty$ to $+\infty$)

$\dot{S}_{t,c}$ First-order derivative of the state

Nomenclature for the ODE model

A Area of oil slick (m^2)

A_{ev} Constant for oil weathering process

A_0 Initial area of slick (m^2)

AC Asphaltene content (%) of the parent oil

B_{ev}	Constant for oil weathering process
C_3	Constant for oil weathering process
C_4	Constant for oil weathering process
F_E	Fraction of oil evaporated
g	Acceleration of gravity (m/s^{-2})
K_1	Constant for oil weathering process
k_2	Constant for oil weathering process
k_3	Constant for oil weathering process
K_{ev}	Constant for oil weathering process
tf_1	Time when the oil spillage stops (release duration)
tf_2	Time at the end of the planning horizon (the end of the planning horizon)
T_G	Gradient of the oil distillation curve
T_K	Temperature (K)
T_O	Initial boiling point of oil
V	Volume of oil slick (m^3)
V_0	Initial volume of oil spilled before time 0
V_D	Volume of oil naturally dispersed
VI	Time-dependent oil spill rate
$WIND$	Wind speed
Y_W	Fraction of water content in the emulsion
v_w	Kinematic viscosity of seawater
ρ_w	Seawater density
ρ_o	Oil density
μ	Viscosity of oil slick
μ_0	Viscosity of parent oil
ζ_t	Oil-water interfacial tension (dynes/m)

References

1. NOAA *Oil spill case histories 1967-1991: summaries of significant U.S. and international spills*; Seattle, Washington, 1992.
2. http://www.restorethegulf.gov/.
3. http://www.deepwaterhorizonresponse.com/.
4. Wilhelm WE, Srinivasa AV. Prescribing tactical response for oil spill clean up operations. Management Science. 1997; 43:386-402.
5. Reed M, Johansen I, Brandvik PJ, Daling P, Alun Lewisà, Fioccoà R, Mackay D, Prentki R. Oil spill modeling towards the close of the 20th century: overview of the state of the art. Spill Science & Technology Bulletin. 1999; 5:3-16.
6. Brebbia CA. Oil spill modeling and processes. WIT Press: UK, 2001.
7. Fingas M. The basics of oil spill cleanup. Lewis: New York, 2001.
8. Ornitz B, Champ M. Oil spills first principles: prevention and best response. Elsevier: Netherlands, 2003.
9. Mackay D, Buist IA, Mascarenhas R, Paterson S *Oil spill processes and models: Environment Canada Manuscript Report No 8. EE-8*; Ottawa, Ontario, 1980.
10. Reed M. The physical fates component of the natural resource damage assessment model system. Oil & Chemical Pollution. 1989; 5:99-123.
11. Zhong Z, You F. Oil spill response planning with consideration of physicochemical evolution of the oil slick: A multiobjective optimization approach. Computers & Chemical Engineering. 2010:Submitted.
12. Fay JA. The spread of oil slicks on a calm sea. In Oil on the sea, Hoult D-P, Ed. Plenum Press: New York, 1969; pp 53-63.
13. Sebastiao P, Sores CG. Modeling the fate of oil spills at sea. Spill Science & Technology Bulletin. 1995; 2:121-131.
14. Stiver W, Mackay D. Evaporation rate of spills of hydrocarbons and petroleum mixtures. Environmental Science & Technology. 1984; 18:834-840.
15. Buchanan I, Hurford N. Methods for predicting the physical changes in oil spilt at sea. Oil & Chemical Pollution. 1988; 4:311-328.
16. Ventikos NP, Vergetis E, Psaraftis HN, Triantafyllou G. A high-level synthesis of oil spill response equipment and countermeasures. Journal of Hazardous Materials. 2004; 107:51–58.

17. Michel J, Adams EE, Addassi Y, Copeland T, Greeley M, James B, Mcgee B, Mitchelmore C, Onishi Y, Payne J, Salt D, Wrenn B. Oil spill dispersants: efficacy and effects. National Academies Press: Washington, DC, 2005.
18. You F, Grossmann IE. Design of responsive supply chains under demand uncertainty. Computers & Chemical Engineering. 2008; 32:2839-3274.
19. You F, Grossmann IE. Balancing responsiveness and economics in the design of process supply chains with multi-echelon stochastic inventory. AIChE Journal. 2009; In press:DOI: 10.1002/aic.12244.
20. You F, Grossmann IE. Stochastic inventory management for tactical process planning under uncertainties: MINLP model and algorithms. AIChE Journal. 2010; In press:DOI: 10.1002/aic.12338.
21. Sager S, Bock HG, Diehl M. The integer approximation error in mixed-integer optimal control. Mathematical Programming. 2010; Accepted.
22. Allgor R, Barton P. Mixed-integer dynamic optimization. Computers & Chemical Engineering. 1997; 21:S451-S456.
23. Allgor R, Barton P. Mixed-integer dynamic optimization I: problem formulation. Computers & Chemical Engineering. 1999; 23:567-584.
24. Bansal V, Sakizlis V, Ross R, Perkins J, Pistikopoulos E. New algorithms for mixed-integer dynamic optimization. Computers & Chemical Engineering. 2003; 27:647-668.
25. Oldenburg J, Marquardt W, Heinz D, Leineweber D. Mixed-logic dynamic optimization applied to batch distillation process design. AIChE Journal. 2003; 49:2900-2917.
26. Sakizlis V, Perkins J, Pistikopoulos E. Recent advances in optimization-based simultaneous process and control design. Computers & Chemical Engineering. 2004; 28:2069-2086.
27. Barton P, Lee C. Design of process operations using hybrid dynamic optimization. Computers & Chemical Engineering. 2004 28:955-969.
28. Chachuat B, Singer A, Barton P. Global mixed-integer dynamic optimization. AIChE Journal. 2005; 51:2235-2253.
29. Chachuat B, Singer AB, Barton PI. Global methods for dynamic optimization and mixed-integer dynamic optimization. Industrial & Engineering Chemistry Research. 2006; 45:8373-8392.
30. Bansal V, Perkins J, Pistikopoulos E. A case study in simultaneous design and control using rigorous, mixed-integer dynamic optimization models. Industrial & Engineering Chemistry Research. 2002; 41:760-778.
31. Giovanoglou A, Barlatier J, Adjiman C, Pistikopoulos E, Cordiner J. Optimal solvent design for batch separation based on economic performance. AIChE Journal. 2003; 49:3095-3109.
32. Low K, Sorensen E. Simultaneous optimal configuration, design and operation of batch distillation. AIChE Journal. 2005; 51:1700-1713.
33. Flores-Tlacuahuac A, Grossmann IE. Simultaneous cyclic scheduling and control of a multiproduct CSTR. Industrial & Engineering Chemistry Research. 2006; 45:6698-6712.
34. Flores-Tlacuahuac A, Biegler LT. Simultaneous mixed-integer dynamic optimization for integrated design and control. Computers & Chemical Engineering. 2007; 31:588-600.
35. Dua P, Dua V, Pistikopoulos EN. Optimal delivery of chemotherapeutic agents in cancer. Computers & Chemical Engineering. 2008; 32:99-107.
36. Flores-Tlacuahuac A, Biegler LT. Integrated control and process design during optimal polymer grade transition operations. Computers & Chemical Engineering. 2008; 32:2823-2837.
37. Prata A, Oldenburg J, Kroll A, Marquardt W. Integrated scheduling and dynamic optimization of grade transitions for a continuous polymerization reactor. Computers & Chemical Engineering. 2008; 32:463-476.
38. Leipold M, Gruetzmann S, Fieg G. An evolutionary approach for multi-objective dynamic optimization applied to middle vessel batch distillation. Computers & Chemical Engineering. 2009; 33:857-870.
39. Flores-Tlacuahuac A, Grossmann IE. Simultaneous scheduling and control of multiproduct continuous parallel lines. Industrial & Engineering Chemistry Research. 2010; 49:7909-7921.
40. Biegler LT. Optimization strategies for complex process models. Advances in Chemical Engineering. 1992; 18:197-256.
41. Byrd RH, Nocedal J, Waltz RA, Knitro: An integrated package for nonlinear optimization. In http://www.ziena.com/papers/integratedpackage.pdf, 2006.
42. Clark P, Westerberg A. Optimization for design-problems having more tha none objective. Computers & Chemical Engineering. 1983; 7:259-278.

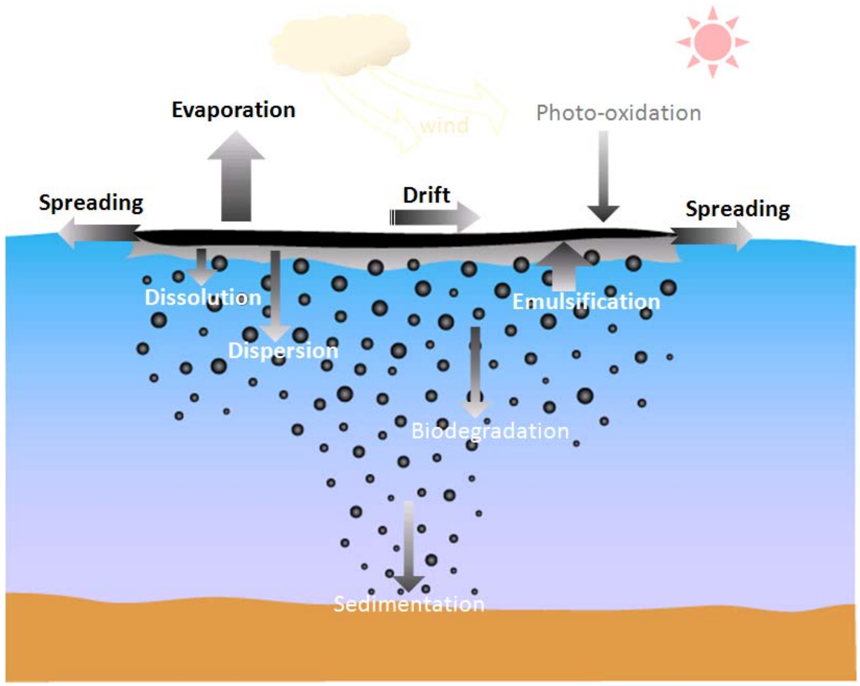

Figure 1. Major oil transport and weathering process

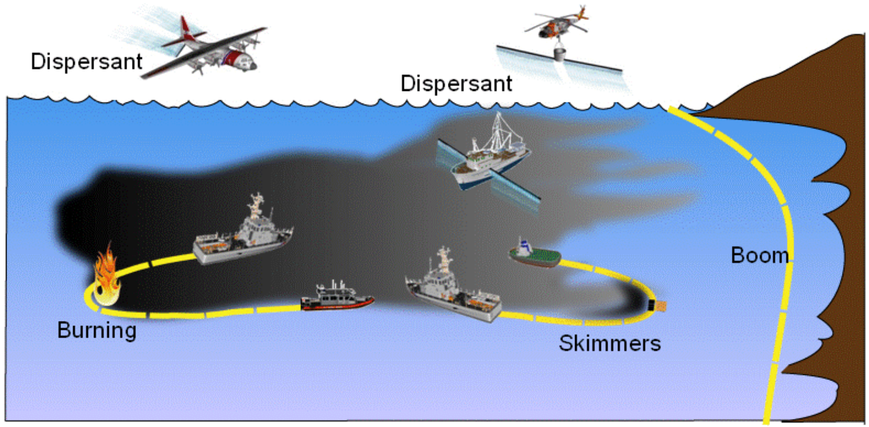

Figure 2. Oil spill cleanup and coastal protection operations

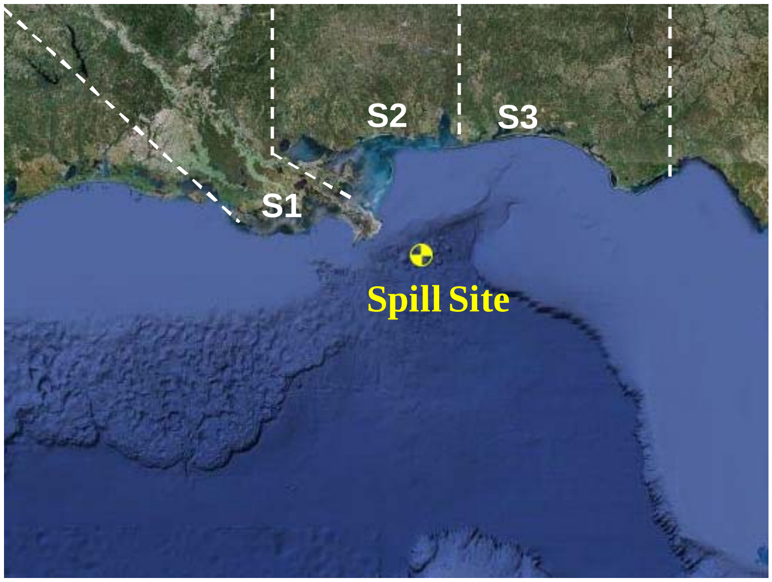

Figure 3. Oil spill site and locations of the three staging areas S1, S2, and S3 for the case study

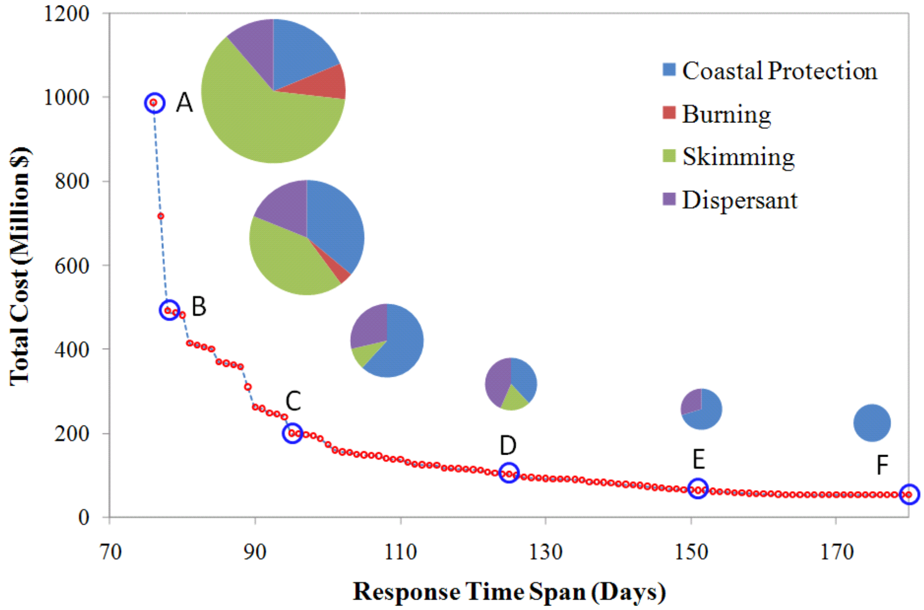

Figure 4. Pareto curve and cost breakdown for case study 1

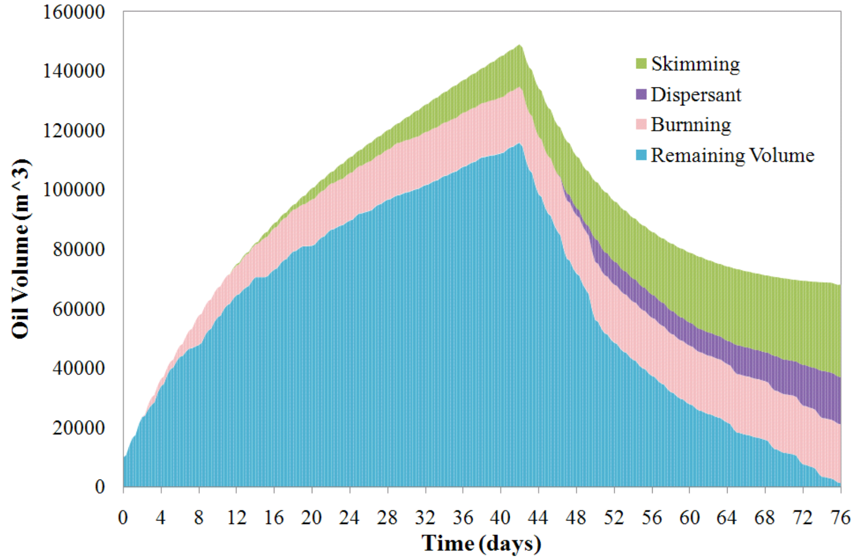

Figure 5. Time trajectories of the oil volumes removed by three methods and remaining on the sea surface when the response time span is 76 days (Point A in Figure 4, drop lines are for the collocation points in the finite elements)

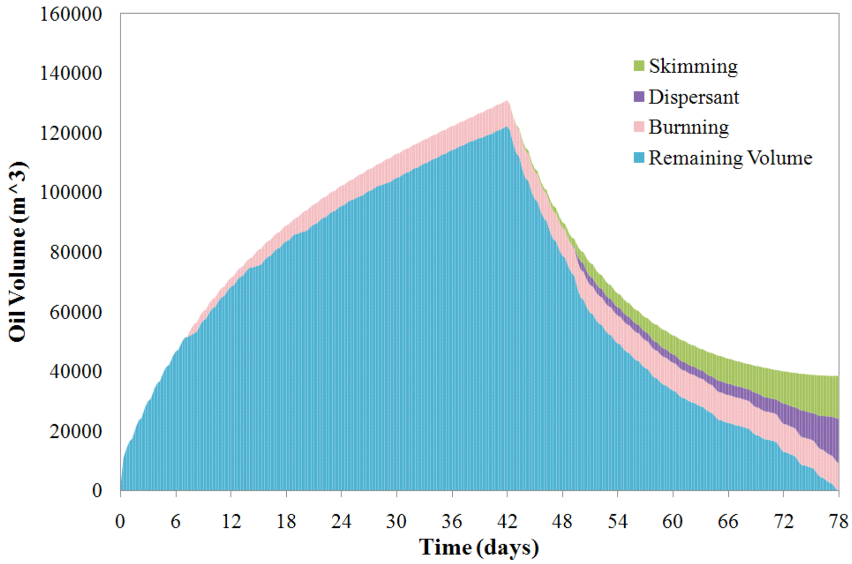

Figure 6. Time trajectories of the oil volumes removed by three methods and remaining on the sea surface when the response time span is 78 days (Point B in Figure 4, drop lines are for the collocation points in the finite elements)

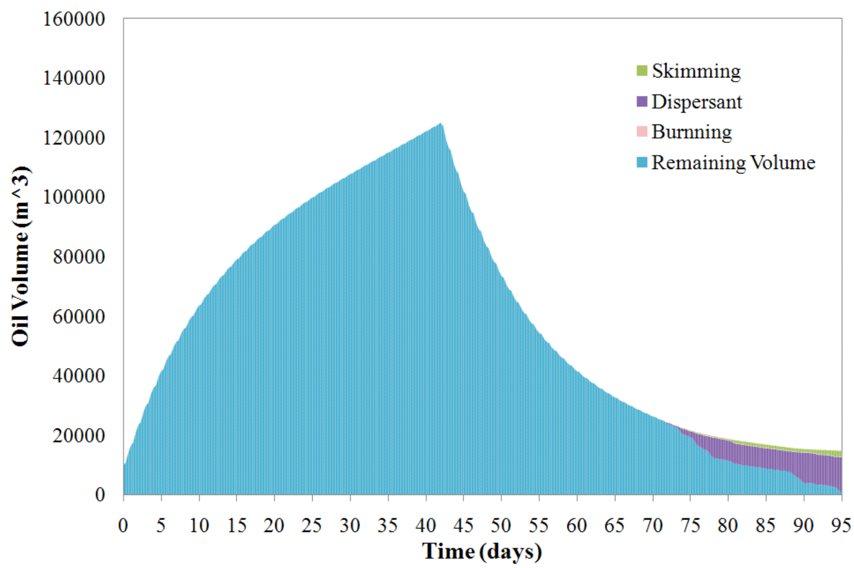

Figure 7. Time trajectories of the oil volumes removed by three methods and remaining on the sea surface when the response time span is 95 days (Point C in Figure 4, drop lines are for the collocation points in the finite elements)

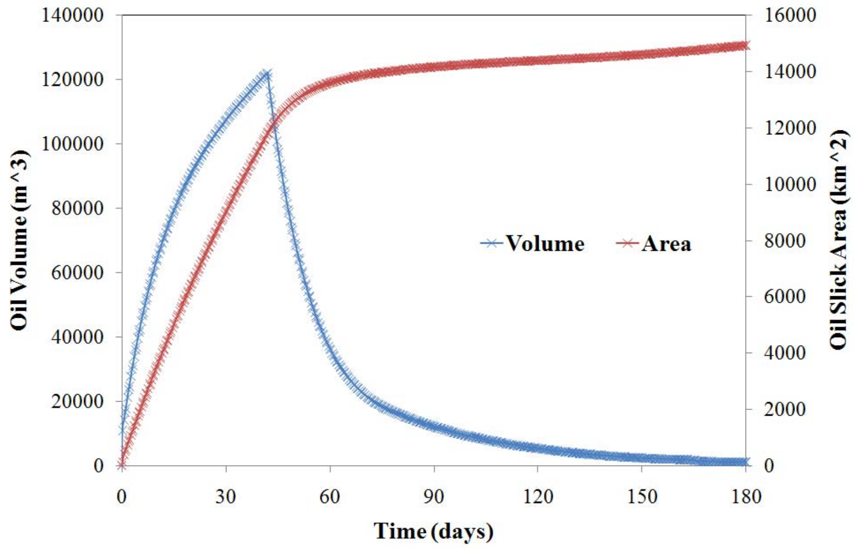

Figure 8. Time trajectories of the oil volumes and area on the sea surface when the response time span is 180 days (Point F in Figure 4, markers are for the collocation points in the finite elements)

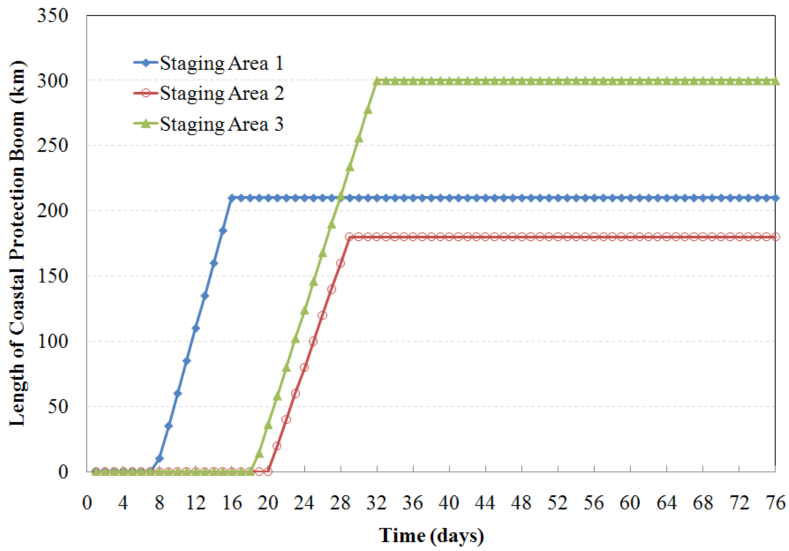

Figure 9. Optimal length of coastal protection boom when response time span is 76 days